SAND2022-7211C

Uncertainty in Annual Energy Resulting from Uncertain Irradiance Measurements

Clifford W. Hansen[1], Aaron Scheiner[2]

1 Sandia National Laboratories, Albuquerque, NM 87185-1033, USA.

2 Rutgers University, New Brunswick, NJ 08901, USA

Abstract— **We report an analysis quantifying the contribution to uncertainty in annual energy projections from uncertainty in ground-measured irradiance. Uncertainty in measured irradiance is quantified for eight instruments by the difference from a well-maintained, secondary standard pyranometer which is regarded as truthful. We construct a statistical model of irradiance uncertainty and apply the model to generate a sample of 100 annual time series of irradiance for each instrument. The sample is propagated through a common performance model for a reference photovoltaic system to quantify variation in annual energy. Although the measured irradiance varies from the reference by a few percent (standard deviation of 1-2%) the uncertainty in annual energy is on the order of a fraction of one percent. We propose a model for a factor that represents uncertainty in modeled annual energy that arises from uncertainty in ground-measured irradiance.**

Keywords— photovoltaic, energy modeling, uncertainty

I. Introduction

Financing institutions often require engineers to estimate uncertainty in projected annual energy for a proposed photovoltaic (PV) energy system in order to establish the project's risk of loan repayment. Annual energy production is estimated by applying a sequence of models to weather data (e.g., irradiance, air temperature) representative of the proposed system's location and operating condition. Uncertainty in annual energy production arises from uncertainties in the weather data, models or system characteristics.

The uncertainty in annual energy is often estimated by applying multipliers to a base estimate of annual energy (e.g. [1]) although more complex methods have been proposed (e.g. [2]). Here we consider the approach outlined in [1] as a practical approach to quantifying uncertainty in annual yield Y:

$$Y = [\sum_t f(\boldsymbol{W}(t), \boldsymbol{P})] \times \prod_{i=1}^{M}(1 - \Delta_i) \qquad (1)$$

In Eq. 1, f represents a performance model for the PV system of interest, $\boldsymbol{W}(t)$ is a time-indexed vector of weather inputs representing a typical or base year, $\boldsymbol{P}$ is a vector of parameters for the performance model. The summation of $f(\boldsymbol{W}(t), \boldsymbol{P})$ provides the annual energy yield for the base year. Uncertainty in this deterministic quantity is described by a set of uncertainty factors, Δ_i, each of which represents the contribution to uncertainty in annual yield of an independent process, parameter or data source. Each factor Δ_i is quantified as a fraction of annual energy yield. When each Δ_i is regarded as a random variable, Y is also a random variable and the result of Equation 1 is a distribution of annual energy yield.

In this paper, we quantify a factor Δ_i representing uncertainty in projected annual energy arising from uncertainty in ground-measured global horizontal irradiance (GHI).

II. Data Source and Data Preparation

We downloaded measured GHI for calendar year 2020 for a total of nine instruments (Table 1) at the National Renewable Energy Laboratory's (NREL) Solar Radiation Research Laboratory in Golden, CO, USA, from the Measurement and Instrumentation Data Center (MIDC [3]. Each GHI instrument is regularly calibrated and maintained and is located in close proximity to all other instruments. We regard these GHI data as among the best achievable measurements for each type of instrument. In addition, we downloaded measured diffuse horizontal irradiance (DHI) measured by a horizontal Kipp and Zonen CMP22 pyranometer with a shade ball, direct normal irradiance (DNI) measured by a Kipp and Zonen DHP1 pyrheliometer, snow depth (cm), precipitation (cm) and air temperature (°C).

One instrument, a Kipp and Zonen CMP22 pyranometer is selected and regarded as the "true" value of GHI. This selection is somewhat arbitrary and not critically important, because our intent is to quantify the effect on annual energy projections of variation of other GHI instruments from the reference. Table I lists the selected irradiance instruments, and the mean and standard deviation of the percent difference in GHI at each time relative to the reference instrument. Instruments are grouped by accuracy class and classes are listed in order of decreasing accuracy. Two other CMP22 instruments (CMP22-1 and CMP22-2) are included, as well as two Licor 200 pyranometers, one of which has a custom temperature adjustment (LI-200R). Nomenclature follows that used by the MIDC to aid in reproducing our analysis. Statistics in Table 1 are not weighted by irradiance and thus a mean difference of e.g. −0.28% for the LI-200 instrument does not imply that the annual insolation would differ by the same percent. Relative differences in GHI are generally more variable for instruments of lower accuracy (Figure 1).

TABLE I. SUMMARY OF GHI INSTRUMENTS AND RELATIVE DIFFERENCES FROM REFERENCE

Instrument	Mean	St. Dev.	Comments
CMP22	-	-	Reference, sec. standard
CMP22-1	0.335%	1.087%	Sec. standard
CMP22-2	0.191%	1.046%	Sec. standard
PSP	0.208%	1.989%	Sec. standard
SPP	0.136%	1.219%	Sec. standard
CMP11	−0.439%	1.422%	Class A
SPLite2	1.03%	1.930%	Economical
LI-200R	0.533%	1.852%	Economical
LI-200	−0.277%	2.323%	Economical

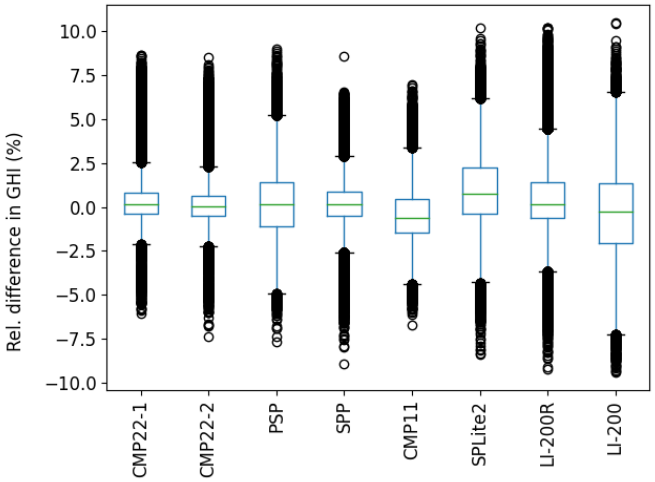

Fig. 1. Relative differences from reference GHI for each instrument.

Data are recorded at 1-minute intervals. For quality checking we also downloaded diffuse horizontal irradiance (DHI for the "Diffuse CMP22-2" instrument), direct normal irradiance (DNI for the "Direct CHP1-1" instrument), solar zenith, precipitation (mm), and snow depth (cm). From the full year of data, we selected the subset where:

- Solar elevation exceeds 5 degrees.
- Recorded GHI is within 5% of GHI estimated as DHI + DNI × cos(Z), where Z is solar zenith.
- Snow depth is 0 cm, and precipitation is less than 2 mm.

These criteria select data where it is unlikely that shadows or other external factors cause differences between instruments.

III. METHODOLOGY

Uncertainty is present in each measurement of GHI in an instrument's time series. Our goal is to understand how the uncertainty in these measurements translates to uncertainty in annual AC energy for a PV system.

To elucidate the uncertainty in annual AC energy, for each instrument we construct many simulated time series of GHI with statistics consistent with the single, measured time series of GHI. We define a reference PV system and a performance model for the system. Keeping all other model inputs (e.g. air temperature) the same for each instrument, the simulated time series of GHI provide an estimate of the distribution of annual AC energy.

To simulate time series of GHI for each instrument, we create a model for the relative difference in GHI between each instrument and the reference GHI. The model ensures that simulated time series have similar distributions of values and similar long-memory autocorrelation that is observed in the measurements. For each instrument k the uncertainty propagation is done as follows:

Step 1: Compute the relative difference $X_k(t)$ in GHI from the reference instrument (subscript R):

$$X_k(t) = (G_k(t) - G_R(t)) / G_R(t) \quad (1)$$

Step 2: Bin the relative differences $X_k(t)$ by irradiance $G_k(t)$ (in increments of 100 W/m^2), air temperature (in increments of 10°C) and solar zenith (in increments of 10 degrees). Within each bin, fit an empirical cumulative distribution function (ECDF). Record each GHI value's rank (percentile) within the appropriate bin's ECDF. Binning is necessary because the distribution of relative difference depends on GHI, air temperature and zenith (e.g., Figure 2). The rank transformation allows for simulations that transition between bins.

Step 3: Use the logit function to transform each rank from the range [0, 1] to $(-\infty, \infty)$ to avoid having constraints on fitting of the time series model.

Step 4: Fit an autoregressive fractionally integrated moving average (ARFIMA) model to the time series of transformed ranks, using the `arfima` function in the R package `forecast` version 8.15[1]. The ARFIMA form is chosen because the time series of relative differences exhibits autocorrelation at long lags (Figure 3). Model order is selected automatically by the `arfima` function.

Step 5: Generate a sample of 100 independent time series of synthetic transformed ranks, and invert the logit and rank transformations and use Eq. 1 to recover 100 independent time series of synthetic GHI, $\tilde{G}_{k,i}(t), i = 1,\ldots,100$.

Step 6: Simulate annual energy $E_{AC,k}(t)$ for each synthetic time series $\tilde{G}_{k,i}(t)$ for a reference PV system at Golden, CO, USA. The reference system is set at 35-degree tilt, azimuth 180°, 1 kW$_{DC}$ and 1 kW$_{AC}$ capacities, with a power temperature coefficient of −0.4%/°C. Simulations are done with pvlib-python [4]. DC and AC output are modeled using functions based on the PVWatts v5 model. Cell temperature is modeled using the Sandia Array Performance Model (SAPM) and coefficients representative of a glass-polymer module on open racking.

Step 7: Compute the relative difference between $E_{AC,k}(t)$ and the annual energy simulated for the reference system using the reference GHI:

[1] https://pkg.robjhyndman.com/forecast/

$$D_k(t) = (E_{AC,k}(t) - E_{AC,R}(t)) / E_{AC,R}(t) \quad (1)$$

The mean and standard deviation of $D_k(t)$ describe the uncertainty in annual energy arising from uncertainty in the GHI measurements for instrument k.

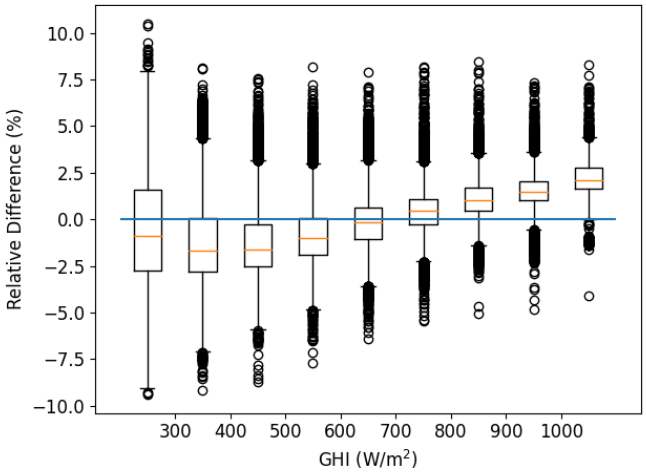

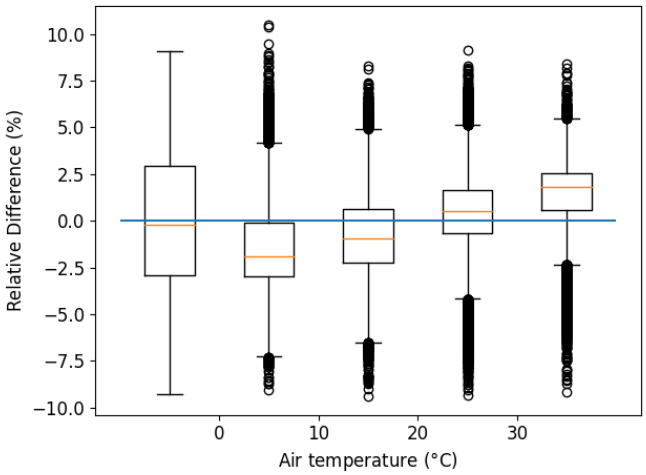

IV. Verification of GHI Simulations

We compared statistics for the relative difference in GHI for the simulations to statistics for the relative difference in observed GHI. Figure 3 shows that autocorrelation matches closely to about lag 10; beyond lag 10 the simulated GHI's autocorrelation exceeds that of the observations. Greater autocorrelation at long lags will tend to overestimate somewhat the variance in annual energy, because the simulated GHI will tend to change less rapidly than the observed GHI and thus remain away from central values for longer periods. We compared the distributions of the relative difference in GHI within each irradiance, temperature and zenith bin (e.g., Figure 4). The distributions are similar for the simulated and observed GHI. These comparisons verify that the statistical model produces GHI time series with statistics that are consistent with the measurements.

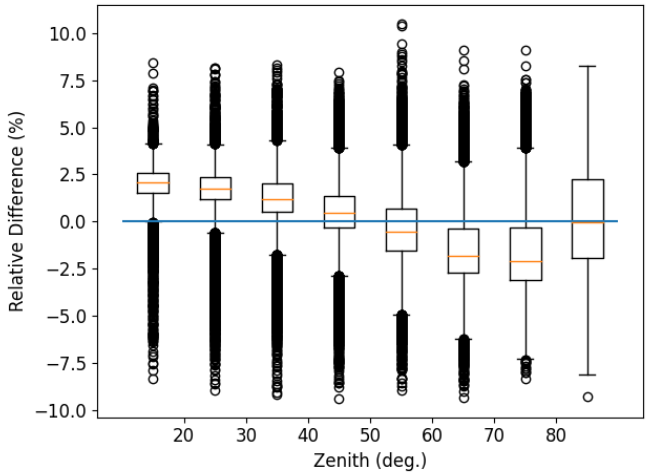

Fig. 2. Relative differences in GHI binned by a) GHI b) air temperature and c) solar zenith for the LI-200 instrument.

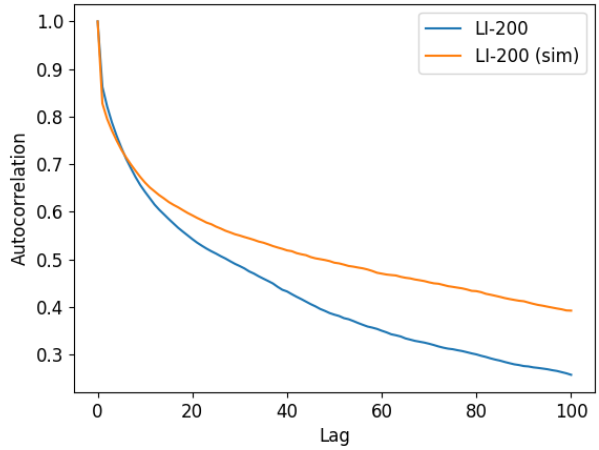

Fig. 3. Autocorrelations for the relative difference in GHI for the LI-200 instrument and for one simulated time series of GHI.

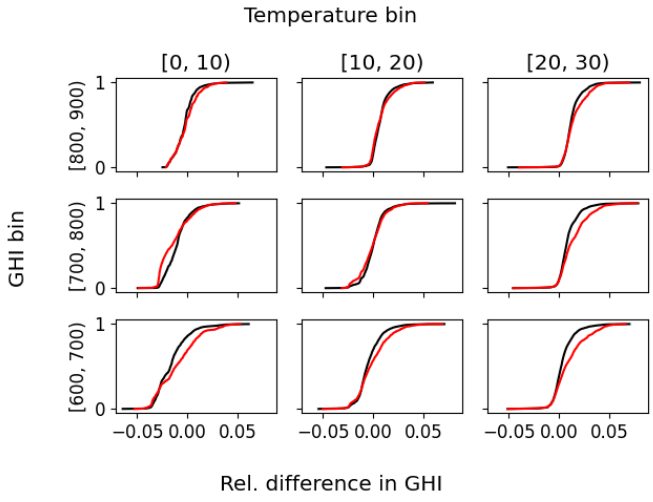

Fig. 4. Distributions of relative difference in GHI: measured (black) and simulated (red) for the LI-200 instrument.

V. Results

Table II summarizes statistics for the distribution of relative difference in AC energy computed for each instrument from the 100 simulated time series of GHI. For each instrument, the distribution of relative difference in AC energy is well-described by a normal distribution (e.g., Figure 5). Confidence intervals indicate that variation among instruments is greater than the uncertainty due to the Monte Carlo generation of simulated GHI time series. Mean relative difference in AC energy is comparable in magnitude to and roughly correlated with the mean relative difference in irradiance (Figure 6a). The correlation is expected because of the strong correlation between insolation (integrated irradiance) and annual AC energy. Interestingly, the mean relative differences for instruments in higher accuracy classes (CMP22-1, CMP22-2, PSP and SPP) are similar to those for economical pyranometers. We hypothesize that this similarity results from careful and accurate calibration of each instrument to a common baseline. The similarity is noteworthy given the conventional wisdom that lower confidence should be assigned to data collected with economical pyranometers, even with proper calibration and maintenance. Even with proper calibration, variation among two pairs of similar instruments (CMP22-1 and CMP22-2, and LI-200 and LI-200R) indicates that instrument calibration or inherent differences can be as great as the variation between instruments of different manufacture.

TABLE II. Summary of Relative Differences in AC Energy

Instrument	Mean	St. Dev.
CMP22-1	0.211%	0.218%
CMP22-2	-0.007%	0.271%
PSP	-0.283%	0.515%
SPP	0.316%	0.432%
CMP11	-0.476%	0.469%
SPLite2	0.674%	0.618%
LI-200R	0.212%	0.374%
LI-200	-0.220%	0.559%

Except for the CMP22-1 and CMP22-2 instruments, the standard deviation of relative differences in AC energy (Figure 6b) is comparable for all other instruments. The relatively low magnitude and small variability for the CMP22-1 and CMP22-2 instruments is likely due to their similarity with the CMP22 instrument selected as the reference GHI. Variance in the simulations of AC energy arises primarily from variance in the relative differences from the reference GHI of the subject instrument. The standard deviation in AC energy is roughly 30% of the standard deviation in irradiance. The reduction in variance likely results from the weighting inherent in the calculation of AC energy (i.e., higher irradiance values contribute more to annual AC energy than to lower irradiance values) combined with the smaller variance in relative differences in irradiance at higher irradiance (e.g., Figure 2a).

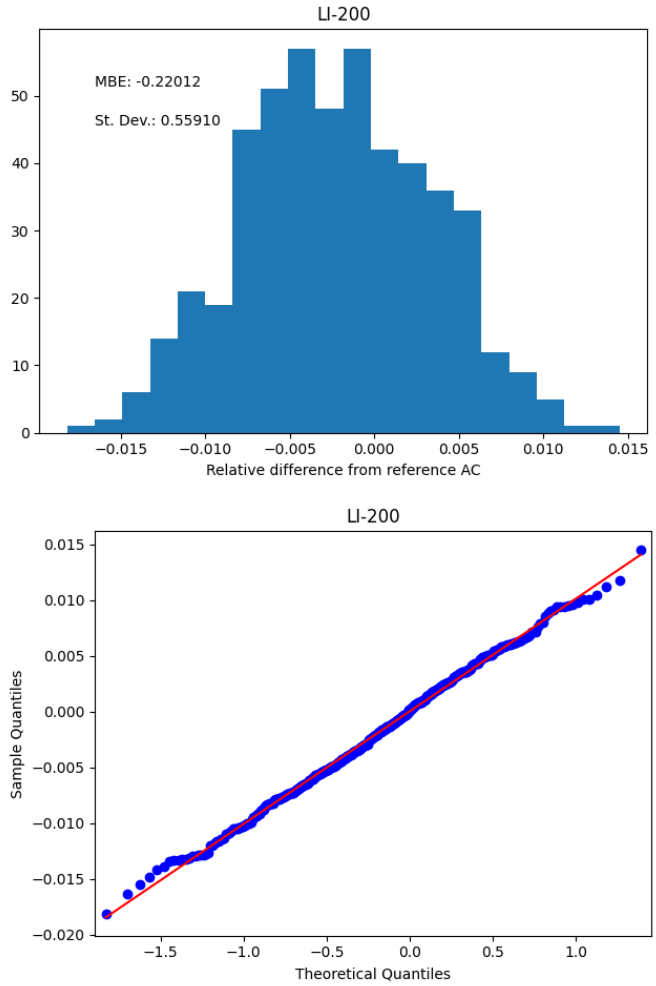

Fig. 5. Distribution of relative difference in AC energy for the LI-200 instrument.

VI. Model for the Uncertainty Factor

We propose the following two-level model for a factor Δ (see Equation 1) which represents uncertainty in annual AC energy resulting from uncertainty in ground-measured irradiance:

- The uncertainty factor Δ is described by a normal distribution.
- The mean of the normal distribution is sampled from a uniform distribution with a range from −0.4% to 0.4%.
- The standard deviation of the normal distribution is sampled from a uniform distribution [0.35%, 0.6%].

The distributions for the mean and standard deviation are defined by excluding the SPLite2 instrument as an outlier in both mean and standard deviation, and by excluding the CMP22-1 and CMP22-2 instruments from the distribution for standard deviation, due to their similarity to the reference GHI instrument. We regard the remaining instruments as representative of all pyranometers with proper calibration. The results in Figure 6 do not appear to support assigning different uncertainty values for higher or lower accuracy instruments.

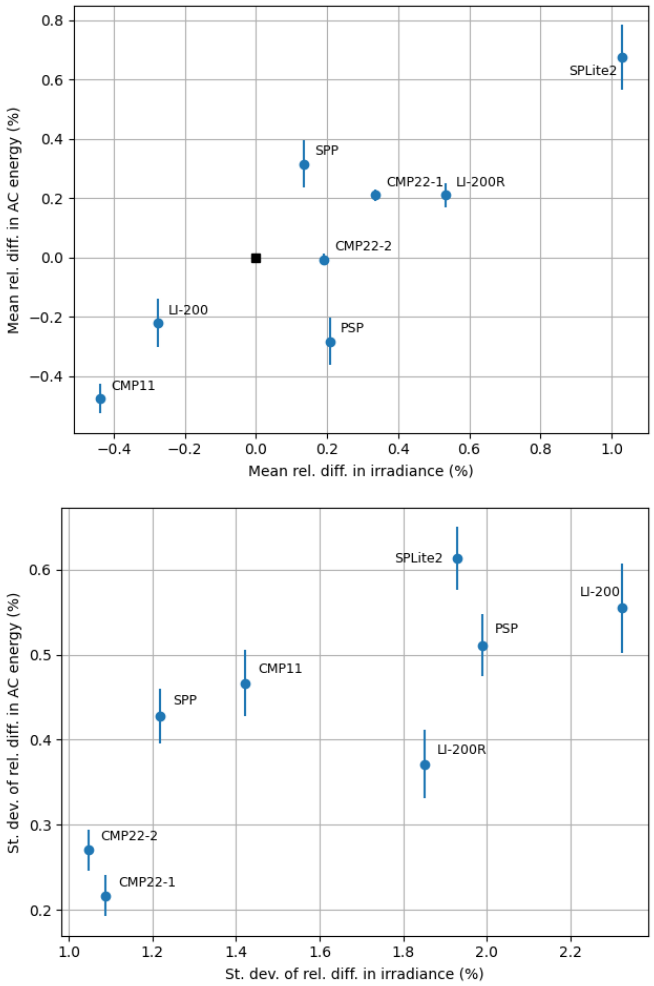

Fig. 6. Mean (a) and standard deviation of relative difference in AC energy compared to relative difference in irradiance. Error bars are confidence intervals (alpha of 0.05) about the overall mean of 5 replicates each of size 100. Error bars indicate uncertainty in overall mean due to sample size.

VII. Summary and Conclusions

Our analysis found that uncertainty in annual AC energy arising from uncertainty in measured GHI can be modeled by a normal distribution. Even for well-calibrated instruments, estimated AC energy can be biased relative to a reference calculation. We found that instruments regarded as less precise (e.g., silicon photodiodes similar to the LI-200) did not necessary correspond with greater uncertainty in annual AC energy. The narrowest uncertain ranges are observed for instruments CMP22-1 and CMP22-2 that are most like the reference CMP22 instrument.

When using an annual factor approach to representing the total uncertainty in AC energy (see Equation 1, and [1] Section 3.2), Table II offers distribution parameters (mean and standard deviation) for several classes of irradiance instruments. However, the distribution means in particular could vary significantly from the mean in Table II when uncertainty in instrument calibration, or instrument to instrument variation, is taken into account. Consequently, we recommend a two-level model for the uncertainty factor, as described in Section VI, that does not distinguish between the type of irradiance instrument.

VIII. Acknowledgment

Sandia National Laboratories is a multimission laboratory managed and operated by National Technology and Engineering Solutions of Sandia, LLC., a wholly owned subsidiary of Honeywell International, Inc., for the U.S. Department of Energy's National Nuclear Security Administration under contract DE-NA-0003525.

IX. References

[1] C. Reise, B. Müller. "Uncertainties in PV System Yield Predictions and Assessments," Intl. Enegy Agency Report IEA-PVPS T13-12:2018, 2018. ISBN 978-3-906042-51-0. 2018.

[2] C. W. Hansen, C. E. Martin. "Photovoltaic System Modeling: Uncertainty and Sensitivity Analyses," Sandia National Laboratories Report SAND2015-6700. 2015.

[3] A. Andreas, T. Stoffel. NREL Solar Radiation Research Laboratory (SRRL): Baseline Measurement System (BMS); Golden, Colorado (Data); NREL Report No. DA-5500-56488. 1981. http://dx.doi.org/10.5439/1052221.

[4] W. F. Holmgren, C. W. Hansen, M. A. Mikofski. "pvlib python: a python package for modeling solar energy systems." Journal of Open Source Software, 3(29), 884, (2018). https://doi.org/10.21105/joss.00884.